CHROMOSPHERIC RESONANCES ABOVE SUNSPOT UMBRAE

G. J. J. Botha[1], T. D. Arber[1], V. M. Nakariakov[1,2], and Y. D. Zhugzhda[3]

[1] Centre for Fusion, Space and Astrophysics, Department of Physics, University of Warwick, Coventry CV4 7AL, UK;
G.J.J.Botha@warwick.ac.uk, T.D.Arber@warwick.ac.uk, V.Nakariakov@warwick.ac.uk
[2] Central Astronomical Observatory of RAS at Pulkovo, 196140 St Petersburg, Russia
[3] Institute of Terrestrial Magnetism, Ionosphere and Radio Wave Propagation, Russian Academy of Sciences, Troitsk, Moscow Region 142190, Russia;
yzhugzhda@mail.ru, yuzef@izmiran.rssi.ru

ABSTRACT

Three-minute oscillations are observed in the chromosphere above sunspot umbrae. One of the models used to explain these oscillations is that of a chromospheric acoustic resonator, where the cavity between the photosphere and transition region partially reflects slow magnetoacoustic waves to form resonances in the lower sunspot atmosphere. We present a phenomenological study that compares simulation results with observations. The ideal magnetohydrodynamic equations are used with a uniform vertical magnetic field and a temperature profile that models sunspot atmospheres above umbrae. The simulations are initialized with a single broadband pulse in the vertical velocity inside the convection zone underneath the photosphere. The frequencies in the spectrum of the broadband pulse that lie below the acoustic cutoff frequency are filtered out so that frequencies equal and above the acoustic cutoff frequency resonate inside the chromospheric cavity. The chromospheric cavity resonates with approximately three-minute oscillations and is a leaky resonator, so that these oscillations generate traveling waves that propagate upward into the corona. Thus, there is no requirement that a narrowband three-minute signal is present in the photosphere to explain the narrowband three-minute oscillations in the chromosphere and corona. The oscillations in the chromospheric cavity have larger relative amplitudes (normalized to the local sound speed) than those in the corona and reproduce the intensity fluctuations of observations. Different umbral temperature profiles lead to different peaks in the spectrum of the resonating chromospheric cavity, which can explain the frequency shift in sunspot oscillations over the solar cycle.

Key words: magnetohydrodynamics (MHD) – Sun: activity – Sun: chromosphere – sunspots

1. INTRODUCTION

Oscillations in and around sunspots can be classified in three broad categories: five-minute oscillations at the photospheric level, three-minute oscillations in the chromosphere above the umbra, and running waves moving away from the umbra along penumbral structures (Bogdan 2000; Bogdan & Judge 2006). This paper will concentrate on the three-minute oscillations, interpreted as slow magnetoacoustic waves moving with the local sound speed along magnetic field lines (e.g., Roberts 2006). The horizontal extent of these oscillations is limited by the umbral size. They are observed from the upper photosphere to the lower corona, with the clearest signal in the chromospheric region. In the transition region, three-minute oscillations are observed in the microwave band as a modulation of gyroresonant emission (Shibasaki 2001), as well as in ultraviolet wavelengths (Marsh et al. 2003). In the corona, these oscillations travel along coronal loops that are anchored in sunspot umbrae (e.g., Brynildsen et al. 2004; De Moortel et al. 2002). A recent review by De Moortel (2009) addresses propagating compressible waves in coronal loops, with observed oscillation periods in the range of 145–550 s. The broadly accepted explanation is that they are waves moving from the photosphere up through the chromosphere into the corona, as this seems to fit most observational data. This is supported by Centeno et al. (2006), who selected the main chromospheric frequency from the photospheric spectrum and showed that an upward moving wave can be fitted to the data. The shortcoming of this model is that the source of the three-minute oscillations at photospheric levels is not well defined. Moreover, Kobanov et al. (2008) showed that the power in the three-minute velocity spectrum is lower in the umbra than the surrounding penumbra at photospheric level, while the oppo-

site is true at chromospheric levels. An alternative explanation is that of a chromospheric acoustic resonator. The photosphere and the temperature gradient of the transition region form the permeable walls of a resonating cavity for slow magnetoacoustic waves (Zhugzhda 2007, 2008). The main criticism against this interpretation is from Brynildsen et al. (2003), who did not detect signals with frequencies corresponding to higher spatial harmonics in a time series of 20 minutes duration. However, the higher spatial harmonics are not necessarily trapped in the resonator. Zhugzhda (2008) pointed out that 20 minutes are not long enough to show the structure of the spectra. By using a temperature that changes non-monotonically with height, Zhugzhda (2008) showed how frequencies below and above the acoustic cutoff frequency behave. Waves above the acoustic cutoff frequency are influenced by the partial reflection from the temperature gradients encountered in the sunspot atmosphere. For waves with frequencies below the acoustic cutoff frequency, the chromosphere resonates at that frequency from the point where the value of the acoustic cutoff frequency drops below the wave frequencies up to the transition region (Taroyan & Erdélyi 2008). Oscillations occurring at the transition region move as traveling waves into the corona. One-dimensional numerical simulations launching waves from the chromosphere (Hansteen et al. 2002) and transition region (Owen et al. 2009) into the corona support the explanation of upward propagating wave trains (Nakariakov et al. 2000). Additional evidence of the leakage of three-minute oscillations into the corona is the recently found relationship between three-minute sunspot oscillations and quasi-periodic pulsations in flaring light curves (Sych et al. 2009).

This paper presents a numerical investigation of the response of the chromospheric resonant cavity to broadband excitation.
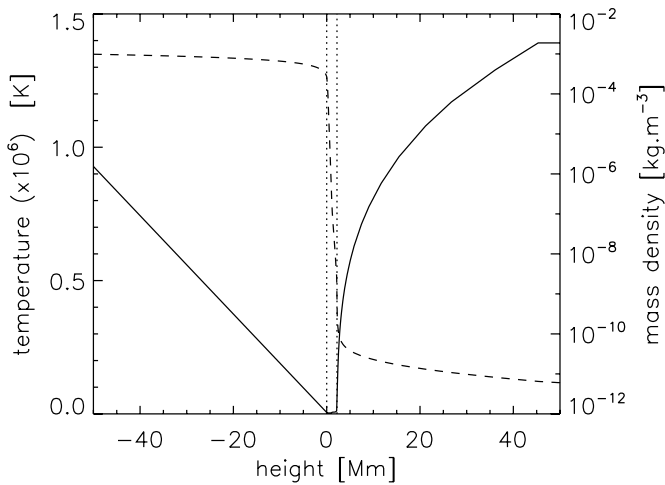
Figure 1. Temperature (solid line) and mass density (broken line) profiles used in the simulations. The photosphere is at height 0 and a polytrope is used below it in the convection zone. The temperature between the photosphere and transition region is taken from the model by Maltby et al. (1986). This distance is indicated by dotted vertical lines and magnified in Figure 2. The coronal temperature above 2.126 Mm is from Avrett & Loeser (2008). Above 45.33 Mm a flat temperature profile is used.

When monochromatic waves are launched from the photosphere into the chromosphere and corona in our simulations, wave trains form that propagate upward, similar to results obtained by Hansteen et al. (2002) and Owen et al. (2009). However, by changing the driver to a single pulse, we are able to study the chromospheric response to broadband excitations. Two cases are investigated: a broadband driver with maximum power below the acoustic cutoff frequency and the other with maximum power above the acoustic cutoff frequency. In both cases, standing waves form in the chromospheric cavity, which leak traveling narrowband waves into the corona. The numerical results do not contradict any of the observations. Hence, we conclude that the chromospheric resonator may play a significant role in the formation of three-minute oscillations.

2. MODEL AND NUMERICAL IMPLEMENTATION

The ideal MHD equations are implemented numerically as described by Arber et al. (2001). Above the sunspot umbra a

vertical magnetic field acts as a guide for slow magnetoacoustic waves moving into the corona. The only role of the magnetic field is that of waveguide, and as such the specific value of the magnetic field strength is not critical. This one-dimensional model ignores the expansion of the flux tube with height. If included, this would lead to lower amplitudes in the oscillations while the structure of the velocity spectra would stay the same. Above the photosphere the chromospheric temperature profile is taken from the sunspot atmospheric model by Maltby et al. (1986) and the coronal temperature is obtained from the model by Avrett & Loeser (2008). Below the photosphere the temperature profile is provided by a polytrope. Figure 1 shows the temperature profile in the numerical domain, while Figure 2 shows an enlargement of the chromospheric region. The mass density in the simulations was obtained by solving the pressure balance equation and its profile is shown in Figure 1. The gravitational acceleration is constant at $g = 274$ m s^{-2}. The photosphere is at the center of the numerical domain, with the bottom and top domain boundaries at ± 68 Mm, respectively. The bottom boundary in the convection zone has line-tied boundary conditions with damping applied to the bottom quarter of the numerical domain. The top boundary in the corona is a Riemann characteristic open boundary that ensures there are no spurious reflections.

The simulation is initialized by a perturbation in the vertical velocity inside the convection zone at a depth of 22.75 Mm below the photosphere. This perturbation is a smooth pulse of the form

$$v_z = \begin{cases} A \, | \cos\left(2\pi t/p\right) - 1 \, | & \text{when} \quad 0 \leqslant t \leqslant p, \\ 0 & \text{when} \quad t > p. \end{cases} \qquad (1)$$

An amplitude of $A = 10^{-4}$ m s^{-1} was used to generate the results presented here. Various values of p were used, of which two are presented in this paper: a two-minute pulse and a five-minute pulse. Figure 3 shows the time evolution of the five-minute pulse, moving both up toward the photosphere and deeper into the convection zone. It shows that the pulse reaches the photosphere after 396 s. Figure 4 shows the time evolution of the fluctuations in the chromospheric region. After the initial pulse has moved through the chromosphere, resonances form after approximately 700 s in this region. The part of the initial
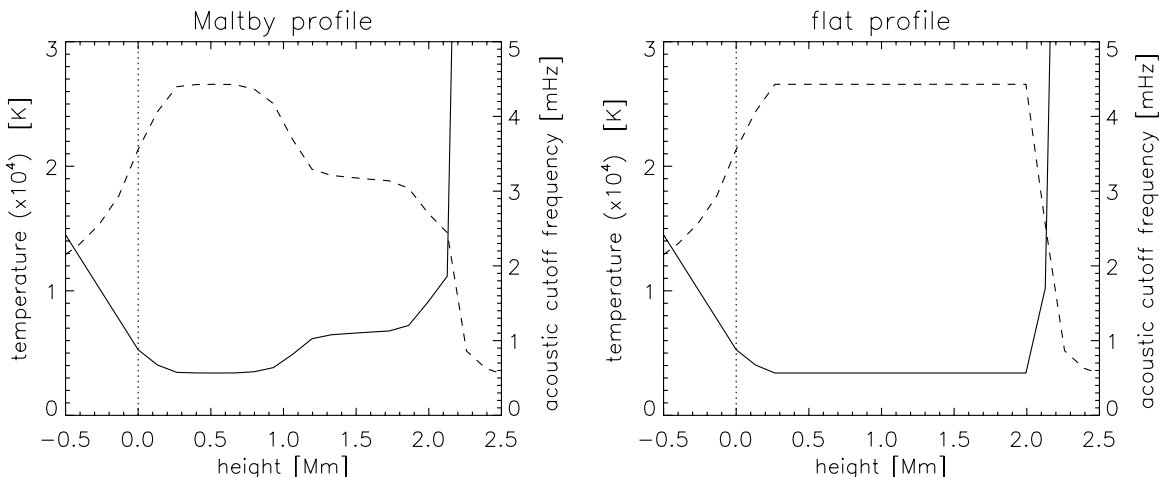
Figure 2. Temperature (solid line) and the acoustic cutoff frequency (broken line) profiles above the sunspot umbra, with the photosphere at height 0. Also shown is an example where the Maltby profile has been replaced with a flat profile. The acoustic cutoff frequency was obtained by using Equation (2) excluding the temperature gradient.
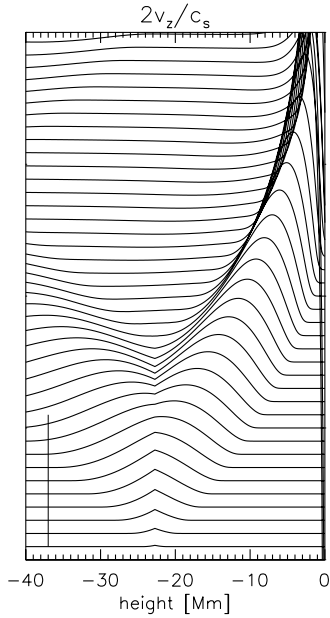
Figure 3. Time evolution of the initial pulse. The amplitude of $2v_z/c_s$ is plotted against height, where v_z is the vertical velocity and c_s is the local sound speed. The vertical line in the bottom left-hand corner shows the scale of an amplitude of 10^{-4}. The first profile at the bottom is at initialization. Every 18 s another profile is plotted to the same amplitude scale, but shifted up from the previous profile. The top profile in the figure is at time 720 s.
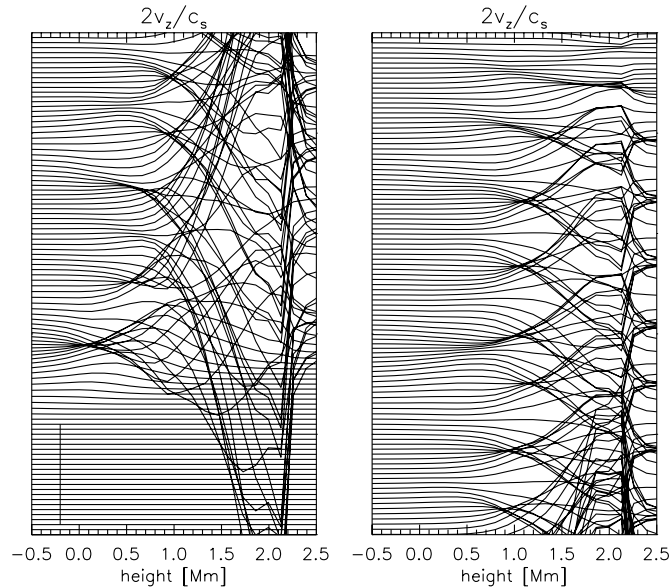
Figure 4. Resonances in the chromospheric cavity. The amplitude of $2v_z/c_s$ is plotted against height, with v_z the vertical velocity and c_s the local sound speed. The vertical line in the bottom left-hand corner shows the scale of an amplitude of 10^{-2}. Every 18 s a profile is plotted, shifted up from the previous profile. The figure on the left-hand side starts at initialization at the bottom and ends at time 1800 s at the top. The figure on the right continues at time 1800 s at the bottom and ends at time 3600 s at the top.

pulse that moves deeper into the convection zone (Figure 3) is damped and does not play a role in the results, as can be seen in Figure 5. After initialization, the plasma at depth 22.75 Mm is free to evolve according to the evolution equations of the model. The initial amplitude of the pulse grows as it moves upward toward the photosphere (Figure 3). When the oscillations reach the photosphere, they are of order m s^{-1}, as shown in Figures 6 and 7.
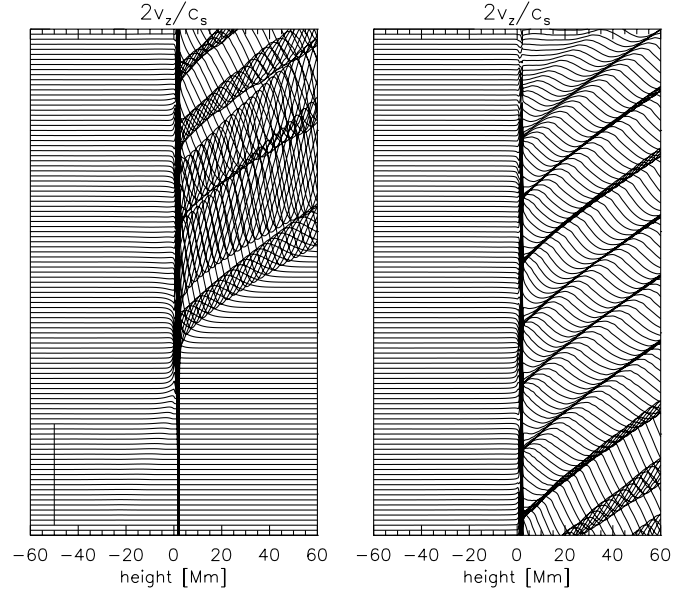
**Figure 5.** Traveling waves moving into the corona. The scale, time step, and layout are the same as in Figure 4.

3. OSCILLATIONS IN THE CHROMOSPHERIC CAVITY

A sunspot's atmosphere can be divided into five layers according to temperature: the photosphere, the temperature minimum, the chromospheric plateau, the transition region, and the coronal temperature. In Figure 2, the photosphere is at height 0, the temperature minimum lies between 0.1 and 0.8 Mm, the plateau between 1.1 and 1.7 Mm, the transition region between 2.0 and 2.2 Mm, and the corona above 2.2 Mm. We shall refer to the region between the photosphere and the transition region as the chromospheric cavity. The acoustic cutoff frequency (ω_c) allows waves to propagate upward with frequencies

$$\omega > \omega_c = \frac{c_s}{2H}\sqrt{1 + 2\frac{\partial H}{\partial z}} \qquad (2)$$

with $H = c_s^2/(\gamma g)$, where γ is the ratio of specific heats, c_s is the sound speed, and z is the height (Roberts 2004). This leads to a local maximum value of 4.43 mHz (3.8 minutes oscillation period) for $\omega_c/2\pi$ at the temperature minimum, as shown in Figure 2. Note that the contribution of $\partial H/\partial z$ in Equation (2) was ignored in Figure 2 even though they are present in the numerical simulations. The gradient of H produces sharp peaks in ω_c approximately between 0 and 0.1 Mm, between 0.9 and 1.1 Mm, and between 0.8 and 2 Mm. These layers are thin compared to the wavelengths of standing waves in the chromospheric cavity and do not influence the result. This was confirmed by using a flat profile in the chromospheric cavity, also shown in Figure 2.

The temperature gradient at the transition region acts as a potential barrier that partially reflects the slow magnetoacoustic waves moving upward. The reflected waves travel down toward the photosphere and are partially reflected at the photospheric temperature gradient, so that a resonance is set up in the chromospheric cavity (Figure 4). In Figure 9, the oscillations are plotted at heights 1.0 Mm, where the local temperature is 4.9×10^3 K, as well as 2.2 Mm (with local temperature 9.0×10^4 K) and 4.9 Mm (with local temperature 5.65×10^5 K). After the initial pulse has moved through the chromospheric cavity, oscillations occur in the chromospheric cavity that are sustained
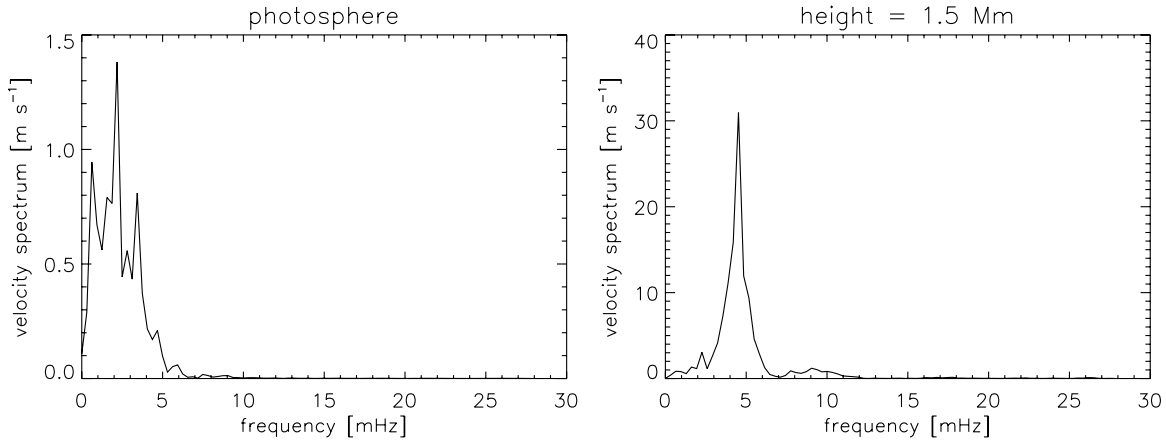
Figure 6. Initialized with a five-minute pulse, the vertical velocity spectra at two different heights are presented. Each data series starts when the velocity amplitude at that height becomes larger than 10^{-4} m s^{-1}. For the spectrum at the photosphere this is at time 396 s and at height 1.5 Mm it is at 504 s. Both data series stop at the end of the run at 3600 s, so that the duration of the time series at the photosphere is 53.4 minutes and at 1.5 Mm 51.6 minutes. The maximum acoustic cutoff frequency is $\omega_c/2\pi = 4.43$ mHz. The dominant frequency at height 1.5 Mm is 4.52 mHz. At the photosphere this frequency is present in the spectrum, but becomes dominant only when the frequencies below max(ω_c) have been filtered out.
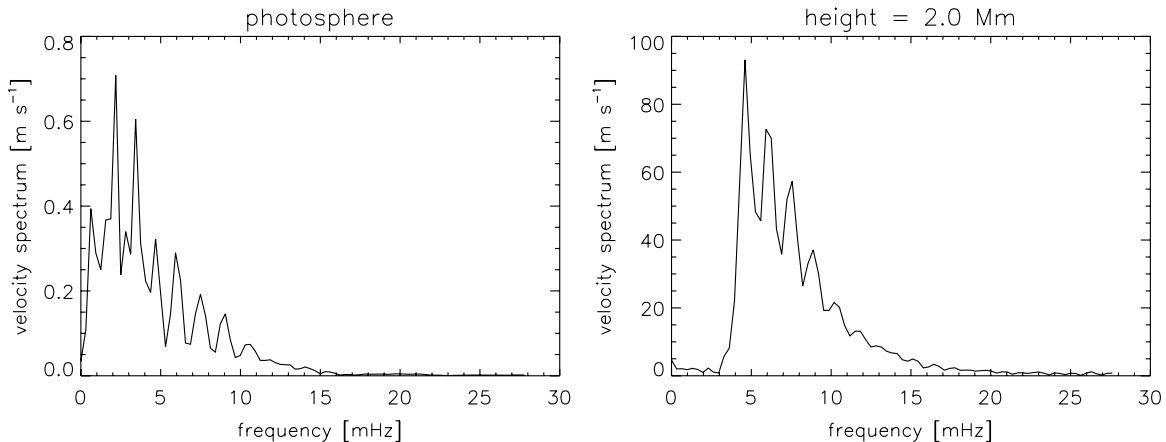
Figure 7. Vertical velocity spectrum at two different heights obtained from a two-minute pulse initialization. Each data series starts when the velocity amplitude at that height becomes larger than 10^{-4} m s^{-1}. For the spectrum at the photosphere this is at time 396 s and at height 2 Mm it is at 558 s. This means the duration of the time series at the photosphere is 53.4 minutes and at 2 Mm 50.7 minutes. The frequency with the largest amplitude at 2 Mm is 4.6 mHz.

for the duration of the numerical run, which was one hour. These oscillations form a standing wave with a clean sinusoidal signature. Figure 9 shows the vertical velocity, normalized to the local sound speed and plotted for heights 1.0 and 2.2 Mm. It is clear that these oscillations are in phase. In order to fit the coronal oscillations on top of those obtained from the chromosphere, the oscillations at 4.9 Mm were shifted backward in time by 45.13 s. This fit shows that the oscillations at the transition region rise into the corona as traveling waves. This is clearly seen in Figure 5. The picture is therefore one in which the chromospheric cavity acts as a leaky resonator.

When the simulation is initialized with a pulse that has a duration of 5 minutes, the frequencies with the most power are below ω_c. The oscillations in the chromospheric cavity that result from this broadband pulse are presented by the velocity spectra in Figure 6. As the pulse moves through the photosphere and the temperature minimum, the frequencies below ω_c are attenuated. Where the temperature rises again above this region, ω_c becomes smaller (Figure 2). At this height, the frequency with the largest amplitude in the spectrum that has survived this evanescent phase starts to grow due to the decreasing density and dominates the spectrum higher in the sunspot's atmosphere. As one would expect, the region with minimum temper-

ature, or equivalently max(ω_c), filters most of the frequencies below ω_c.

The spectra obtained with an initial pulse of two minutes duration are presented in Figure 7. The frequencies in the spectrum above ω_c survive throughout the sunspot's atmosphere and resonate in the chromospheric cavity. The frequencies below ω_c are filtered out of the spectrum in the temperature minimum region. The dominant frequency shifts with height. Figure 7 shows that the photospheric spectrum contains ω_c and its higher harmonics. These harmonics are present but not very pronounced in the spectrum at the top of the chromospheric cavity, as shown at 2.0 Mm in Figure 7. Changing the temperature profile from Maltby to flat (Figure 2) does not change the appearance of these higher harmonics. From the top of the temperature plateau (1.8 Mm) the shape of the spectrum stays the same as one moves higher into the atmosphere. It has the typical form observed for three-minute oscillations above sunspots, namely, a sharp rise below 5 mHz, and a gradual falloff beyond 8 mHz (Bogdan & Judge 2006).

As the broadband pulse moves from the photosphere through the chromosphere, it sets up a sustained oscillation in the chromospheric cavity that has a frequency spectrum that peaks at around three minutes, as shown in Figures 6 and 7. This
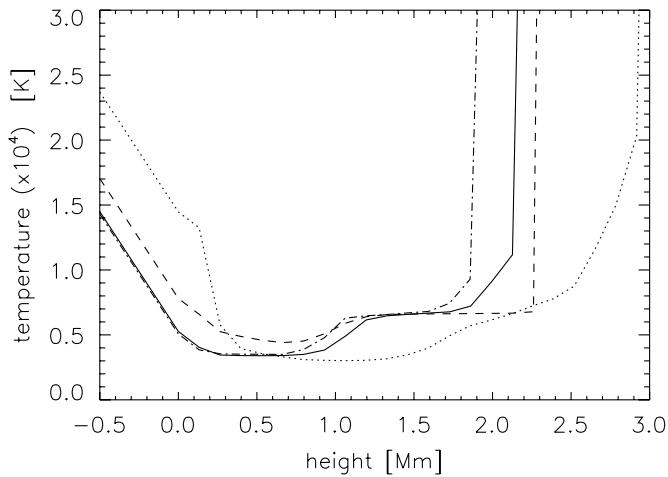
Figure 8. Different temperature profiles used in the simulations: the solid line is from Maltby et al. (1986), the dashed line is the VAL-C quiet-Sun atmosphere (Avrett & Loeser 2008), the dotted line is from Staude (1981), and the dot-dashed line is from Lites & Skumanich (1982). The resonance frequencies obtained in each case are presented in Table 1.

Table 1
Dominant Frequencies for Different Temperature Profiles

Temperature Profile	Two-minute Pulse	Five-minute Pulse
Maltby et al. (1986)	4.55 mHz at 1.5 Mm	4.52 mHz at 1.5 Mm
	4.6 mHz at 2 Mm	4.55 mHz at 2 Mm
Lites & Skumanich (1982)	4.55 mHz at 1.5 Mm	4.52 mHz at 1.5 Mm
	4.6 mHz at 2 Mm	4.55 mHz at 2 Mm
Staude (1981)	6.42 mHz at 1.5 Mm	5.11 mHz at 1.5 Mm
	4.58 mHz at 2 Mm	4.52 mHz at 2 Mm
VAL-C quiet Sun	3.88 mHz at 1.5 Mm	3.85 mHz at 1.5 Mm
	3.92 mHz at 2 Mm	3.9 mHz at 2 Mm
Flat chromosphere (Figure 2)	4.55 mHz at 1.5 Mm	4.52 mHz at 1.5 Mm
	4.63 mHz at 2 Mm	4.58 mHz at 2 Mm

Notes. All velocity spectra were obtained from the time when the amplitude of the vertical velocity becomes $\geqslant 10^{-4}$ m s^{-1} at the height the specific spectrum was taken, until the end of the numerical run at time 3600 s. At height 1.5 Mm the starting time is approximately 500 s and at height 2 Mm it is approximately 540 s.

chromospheric oscillation excites traveling waves that propagate upward into the corona. The shape of the velocity spectrum at the transition region is the same as that at all heights into the corona. The presence of a clear narrowband spectrum, at around the three-minute period, in the corona does not therefore imply that such a narrowband driver is present in the photosphere.

Centeno et al. (2006) took the velocity signal from a low photospheric and a transition region spectral line and filtered them in narrow bands around the three-minute oscillations. By adjusting amplitudes and shifting the signals in time it was shown that these two time series could be fitted on top of each other. The temporal shift, typically around 240 s, was in the direction that supported modulations rising from the photosphere through the chromosphere. This temporal shift is the sound transit time determined from $\int 1/c_s \, dl$ across the chromosphere. Using the results obtained with the five-minute initial pulse, we have followed the same method. Frequencies in the range 4–5 mHz were selected and then time series for the velocity were constructed at various heights in the atmosphere. For heights less than about 1 Mm, there are increasing phase shifts in the signal with increasing height. However above 1 Mm, but below the corona, the phase of the signal remains constant. The lack of phase shift above 1 Mm is consistent with this signal being of a standing wave. Below 1 Mm the phase shift changing with height can be interpreted as a propagating signal. This disagrees with the interpretation in Centeno et al. (2006) where a propagating signal from the photosphere all the way to the transition region was concluded. However, Centeno et al. (2006) only had observations at the photosphere and transition region, and the temporal shift to make the oscillations overlap was greater than the three-minute period of wave oscillation. It is therefore possible that a fit could be constructed with a time shift of, for example, 60 s. This would be the shift applied by Centeno et al. (2006) minus one whole period of the three-minute oscillations. This would then be consistent with the simulations presented here in which there is a shift in phase, i.e., propagating signal, only in the lower atmosphere with a standing wave above.

No shocks formed during the simulations. This is consistent with observations of linear oscillations that are stable over days (Shibasaki 2001). However, Centeno et al. (2009) observed

shocks in atmospheres of large sunspots. In our simulations, the amplitude of the oscillations depends on the amplitude of the initial pulse. Figure 9 shows that both initial pulses lead to an observable amplitude of a few percent in the transition region, in agreement with observations of intensity perturbations in the lower corona (McEwan & De Moortel 2006). The initial oscillations due to the five-minute pulse are smaller than those of the two-minute pulse because more of the five-minute pulse is below ω_c and consequently attenuated in the temperature minimum region. As a result, the five-minute pulse has a smaller signal at resonance. To obtain larger relative amplitudes or shocks, one has to increase the amplitude of the initial pulse (Equation (1)). Figure 9 shows that the normalized oscillation amplitudes decay with time as energy continuously leaks through the transition region into the corona in the form of traveling waves.

Figure 9 also shows that the amplitude of the traveling wave, normalized to the local sound speed, at a coronal height of 4.9 Mm is approximately the same as that of the oscillations in the chromosphere at height 1.0 Mm. As one moves higher up in the chromospheric cavity, the oscillation amplitudes increase so that amplitudes are largest at the top of the chromosphere (2.2 Mm). This numerical result agrees with observations that relative oscillation amplitudes reach a maximum in the transition region, decrease with height up till a coronal temperature of 10^6 K, before increasing again as one moves to higher coronal temperatures (O'Shea et al. 2002).

Different models of the temperature profile in a sunspot atmosphere have different resonant frequencies. Apart from the temperature profile by Maltby et al. (1986) (Figure 2), we have used the models of Lites & Skumanich (1982) and Staude (1981), as well as the quiet-Sun (VAL-C) atmosphere by Avrett & Loeser (2008). The temperature profile was also simplified by using a flat profile in the chromospheric cavity (Figure 2). These temperature profiles are presented in Figure 8. All cases produced qualitatively similar results. The key physical parameters are the height of the whole chromospheric cavity and the location of the temperature minimum, i.e., max(ω_c). As the distance between the photosphere and temperature minimum increases, more attenuation or filtering of the lower frequencies in the spectrum occurs. Also, as the height between photosphere and transition region increases, the resonating spectra shifts to lower frequencies. A comparison of the dominant frequencies in the velocity spectra at two heights above the photosphere is
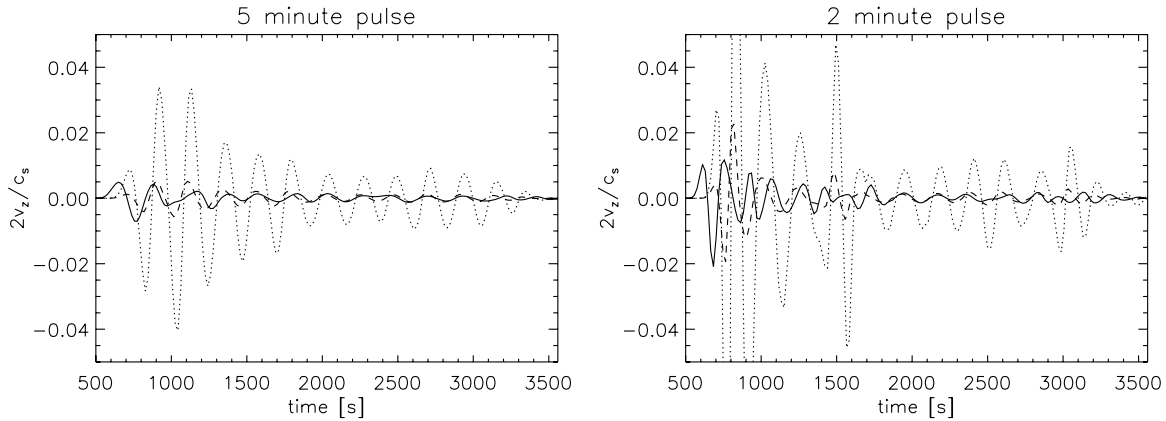
Figure 9. Vertical velocity fluctuations normalized to the local sound speed c_s. On the left are measurements from an initial five-minute pulse and on the right from a two-minute pulse. The solid line represents measurements at height 1.0 Mm, the dotted line 2.2 Mm, and the dashed line 4.9 Mm. A standing wave forms in the chromospheric cavity, while a traveling wave moves from the transition region into the corona. In both cases, the fluctuations measured at 4.9 Mm were shifted backward in time by $\triangle t = L/c_s$ to fit on top of the other two curves, where $L = 2.7$ Mm and c_s is the average sound speed taking only the sound speeds at the transition region (2.2 Mm) and in the corona (4.9 Mm) into account. The other measurements are plotted without any time shifts. The two-minute pulse oscillation amplitudes at 2.2 Mm lie in the interval (-0.125, 0.15) and go out of scale range of the figure.

presented in Table 1. These may be the mechanisms responsible for the frequency shift in the three-minute oscillation during the solar cycle, as observed by Tlatov & Riehokainen (2008). They found that basic three-minute oscillations tend to have higher frequencies during solar minimum and lower frequencies during solar maximum.

Table 1 shows that most of the oscillations in our simulations have periods of around 4.6 mHz at a height of 2 Mm, i.e., a period of 3.6 minutes in the corona. The exception to this is the VAL-C model which gave a dominant coronal period of 4.3 minutes. This is not surprising as the VAL-C model is for the quiet chromosphere, while all the others are for model atmospheres above sunspots. Thus, while all model atmospheres show chromospheric resonance, and it is possible to distinguish active region atmospheres from the VAL-C model, the active region models all have peaked spectra at 3.6 minutes—not the observed 3 minutes. The simplified model used in this paper omits flux tube expansion, radiation and conduction. It has been shown that flux tube expansion reduces the period of Alfvén waves (De Moortel et al. 2000), but it is unlikely that thermal conduction and radiation would effect the period of the oscillation (Macnamara & Roberts 2010). Of course, the period can also be altered by changing the model atmosphere to one with a higher temperature or shorter distance between temperature minimum and transition region.

The Fabry–Perot resonator (Paschotta 2008) was associated with chromospheric resonances by Zhugzhda & Locans (1981), whose calculations showed a complex spectrum covering periods from 1 to 3 minutes (Zhugzhda et al. 1983). In particular, localized layers of enhanced temperature gradients compared to the mean provide additional reflections (Zhugzhda 2008). Although the results presented in this paper were obtained with the Maltby profile, we have performed the same simulations with the VAL-C model, other sunspot atmospheres, and a flat temperature profile, all resulting in qualitatively similar results. No effects were observed due to enhanced temperature gradients in the chromospheric cavity. This is not surprising, given that for three-minute oscillations in an atmosphere at 5×10^3 K, the sound speed is 6 km s^{-1} and the wavelength 1 Mm, which is much longer than the scale lengths of the enhanced temperature gradient layers in the Maltby profile.

4. SUMMARY

Results of the response of a sunspot atmosphere to broadband excitation are presented in this paper: with the input energy mainly below the acoustic cutoff frequency (ω_c) as well as mainly above ω_c. In both cases, standing waves form in the chromospheric cavity, while traveling waves leak into the corona (Figures 4 and 5).

Figure 2 shows that ω_c changes with height. Most of the frequencies in the five-minute pulse are below ω_c at the temperature minimum and are filtered out of the spectrum. Where ω_c becomes smaller, the dominant frequency resonates in the cavity between this point and the transition region. Most of the frequencies in the two-minute pulse are above ω_c. In this case, the dominant physical mechanism is partial reflection from the temperature gradients at the photosphere and in the transition region, so that a resonance is established in the chromospheric cavity. It is possible to differentiate between the two types of broadband pulses by the spectrum of the standing wave in the chromospheric cavity. The five-minute pulse gives an oscillatory response with a single dominant frequency (Figure 6), while the two-minute pulse leads to spectra with a sharp rise below 5 mHz and a gradual falloff above 8 mHz (Figure 7). The latter is consistent with observations (Bogdan & Judge 2006).

The oscillation amplitudes (normalized to the local sound speed) are small enough for the physics to stay linear and no shocks form. These amplitudes are a few percent in the transition region in agreement with observations. Figure 9 shows that the normalized amplitudes in the transition region are larger than those of the wave trains moving into the corona, which are comparable to amplitudes in the lower part of the chromospheric cavity. All amplitudes can be increased by increasing the initial pulse amplitude.

Different temperature profiles have been used, with the results presented in this paper obtained by using the profile in Figure 2. All profiles give qualitatively the same results. The quantitative differences between the profiles allow for the possibility to select the appropriate model for each individual sunspot. Different temperature profiles may also provide an explanation for the frequency changes in the three-minute os-

cillations observed during a solar cycle (Tlatov & Riehokainen 2008).

We conclude that a chromospheric resonator above sunspot umbrae is consistent with existing observations. Results similar to the observations by Centeno et al. (2006) were produced, as well as normalized amplitudes of a few percent in the transition region (McEwan & De Moortel 2006) that are larger than those in the corona (O'Shea et al. 2002). The results demonstrate that three-minute oscillations in the chromospheric cavity are obtained without the need for a clear three-minute source in the photosphere.

REFERENCES

Arber, T. D., Longbottom, A. W., Gerrard, C. L., & Milne, A. M. 2001, J. Comput. Phys., 171, 151
Avrett, E. H., & Loeser, R. 2008, ApJS, 175, 229
Bogdan, T. J. 2000, Sol. Phys., 192, 373
Bogdan, T. J., & Judge, P. G. 2006, Phil. Trans. R. Soc. A, 364, 313
Brynildsen, N., Maltby, P., Brekke, P., Fredvik, T., & Kjeldseth-Moe, O. 2003, Adv. Space Res., 32, 1097
Brynildsen, N., Maltby, P., Foley, C. R., Fredvik, T., & Kjeldseth-Moe, O. 2004, Sol. Phys., 221, 237
Centeno, R., Collados, M., & Trujillo Bueno, J. 2006, ApJ, 640, 1153
Centeno, R., Collados, M., & Trujillo Bueno, J. 2009, ApJ, 692, 1211
De Moortel, I. 2009, Space Sci. Rev., 149, 65
De Moortel, I., Hood, A. W., & Arber, T. D. 2000, A&A, 354, 334
De Moortel, I., Ireland, J., Hood, A. W., & Walsh, R. W. 2002, A&A, 387, L13
Hansteen, V. H., Wikstøl, Ø., Brynildsen, N., Maltby, P., Fredvik, T., & Kjeldseth-Moe, O. 2002, in Proc. SOLMAG 2002: Magnetic Coupling of the Solar Atmosphere Euroconference and IAU Colloq. 188, ed. H. Sawaya-Lacoste (ESA SP-505; Noordwijk: ESA), 183
Kobanov, N. I., Kolobov, D. Y., & Chupin, S. A. 2008, Astron. Lett., 34, 133
Lites, B. W., & Skumanich, A. 1982, ApJS, 49, 293
Macnamara, C. K., & Roberts, B. 2010, A&A, 515, A41
Maltby, P., Avrett, E. H., Carlsson, M., Kjeldseth-Moe, O., Kurucz, R. L., & Loeser, R. 1986, ApJ, 306, 284
Marsh, M. S., Walsh, R. W., De Moortel, I., & Ireland, J. 2003, A&A, 404, L37
McEwan, M. P., & De Moortel, I. 2006, A&A, 448, 763
Nakariakov, V. M., Verwichte, E., Berghmans, D., & Robbrecht, E. 2000, A&A, 362, 1151
O'Shea, E., Muglach, K., & Fleck, B. 2002, A&A, 387, 642
Owen, N. R., De Moortel, I., & Hood, A. W. 2009, A&A, 494, 339
Paschotta, R. 2008, Encyclopedia of Laser Physics and Technology (1st ed.; Berlin: Wiley-VCH), http://www.rp-photonics.com/encyclopedia.html
Roberts, B. 2004, in Proc. SOHO13—Waves, Oscillations and Small-Scale Transient Events in the Solar Atmosphere: A Joint View From SOHO and TRACE, ed. H. Lacoste (ESA SP-547; Noordwijk: ESA), 1
Roberts, B. 2006, Phil. Trans. R. Soc. A, 364, 447
Shibasaki, K. 2001, ApJ, 550, 1113
Staude, J. 1981, A&A, 100, 284
Sych, R., Nakariakov, V. M., Karlicky, M., & Anfinogentov, S. 2009, A&A, 505, 791
Taroyan, Y., & Erdélyi, R. 2008, Sol. Phys., 251, 523
Tlatov, A. G., & Riehokainen, A. 2008, A&A, 487, 1143
Zhugzhda, Y. D. 2007, Astron. Lett., 33, 622
Zhugzhda, Y. D. 2008, Sol. Phys., 251, 501
Zhugzhda, Y. D., & Locans, V. 1981, Sov. Astron. Lett., 7, 25
Zhugzhda, Y. D., Locans, V., & Staude, J. 1983, Sol. Phys., 82, 369